

**GEOLOGIC MAP  
OF THE  
BOREALIS REGION  
(H-1)  
OF MERCURY**

By  
Maurice J. Grolier and Joseph M. Boyce

1984

Prepared for the  
National Aeronautics and Space Administration  
by  
U.S. Department of the Interior, U.S. Geological Survey

(Published in hardcopy as USGS Miscellaneous Investigations Series Map I-1660, as part of the Atlas of Mercury, 1:5,000,000 Geologic Series. Hardcopy is available for sale from U.S. Geological Survey, Information Services, Box 25286, Federal Center, Denver, CO 80225)

Please direct questions or comments about the digital version to:  
Richard Kozak  
U.S. Geological Survey  
2255 N. Gemini Drive  
Flagstaff, AZ 86001  
e-mail: [rkozak@flagmail.wr.usgs.gov](mailto:rkozak@flagmail.wr.usgs.gov)

## DESCRIPTION OF MAP UNITS

### PLAINS MATERIALS

- ps SMOOTH PLAINS MATERIAL—Forms flat to gently rolling plains at resolution of Mariner 10; commonly occurs in low depressions such as Borealis and Suisei Planitiae, in basins such as Goethe (FDS 160), and in large  $c_1$  to  $c_4$  craters (FDS 156). Intermediate albedo. Characterized by sharp or gradational overlapping contacts with older terrain and by sparsity of  $c_1$  to  $c_3$  craters, except for subjacent ghost craters. Sinuous ridges and scarps common. *Interpretation:* Probably lava; no volcanic vents observed. Two very long but discontinuous scarps concentric to Goethe Basin and one circular scarp bounding shieldlike platform around crater Depréz may represent fronts of viscous volcanic lava flows that crossed Borealis Planitia. Alternatively, may consist of fluidized shock-melted material
- psi INTERMEDIATE PLAINS MATERIAL—Forms flat to gently rolling plains north and northeast of Suisei Planitia (FDS 157, 161). Albedo similar to that of smooth plains material. Contains fewer superposed craters than intercrater plains material and more than smooth plains material. Embayment relations with older and younger plains materials unclear, except along western border of Borealis Planitia. *Interpretation:* Uncertain: may consist of impact materials ranging from basin and crater ejecta, similar to some facies in Caloris Basin ejecta, to shock melt and breccia; may also consist in part of volcanic materials. Intermediate crater density may indicate age transitional between intercrater plains and smooth plains materials
- pi INTERCRATER PLAINS MATERIAL—Forms hummocky, pitted, locally grooved and lineated plains mostly west of the  $100^\circ$  meridian (FDS 152, 165). Albedo similar to that of smooth plains and intermediate plains materials. High density of superposed, overlapping craters 5 to 10 km in diameter; most craters elliptical, shallow, and open on one side, superposed on degraded remnants of larger craters. Unit overlaps or overlies rounded rims of ghost craters in Suisei Planitia and north of Goethe Basin. *Interpretation:* May be mixture of basin and crater ejecta and volcanic deposits emplaced during terminal phase of heavy bombardment

### BASIN AND CRATER MATERIALS

- CRATER MATERIALS—Craters  $>30$  km in diameter showing various degrees of degradation and burial. Subscripts refer to degradation sequence from  $c_1$  (most degraded) to  $c_4$  (least degraded). *Interpretation:* Formed by impact. Degree of degradation is assumed to represent relative age ( $c_1$  oldest to  $c_4$  youngest) of craters of closely similar diameters (McCauley and others, 1981)
- $c_4$  Material of craters with scalloped or slightly subdued rims, terraced walls, and terraces disrupted by slumping—Central peak or peaks usually present; sharp contact of wall with floor.

- Interpretation:* Rim material consists of overturned flap and fall-back; upper part of wall is bedrock; slump and colluvium along footwall and base of terraces. Floor consists of brecciated bedrock and fallback ejecta; floors partly flooded with smooth plains material representing impact melt or post-impact lava flows
- cp4 Central peak material of c<sub>4</sub> craters—Peaks either single or more rarely in clusters of multiple peaks that rise above crater floors near their centers (Verdi, FDS 166; Jókai, FDS 161).  
*Interpretation:* Formed by rebound after impact
- cf4 Crater floor material of c<sub>4</sub> craters—Material of some crater floors is hilly, hummocky, or rolling; other crater floors surfaced by smooth plains material. *Interpretation:* Hummocks are blocks of fallback ejecta; smooth surface represents resurfacing by shock melt or lava flows
- cr4 Crater ejecta material, radial—Forms well-developed, radially linedated, distinctive annulus adjacent to rims of large c<sub>4</sub> craters. *Interpretation:* Ballistically emplaced ejecta, mixed with precrater material: the small-crater equivalent of linedated facies of Van Eyck Formation (McCauley and others, 1981) surrounding Caloris Basin
- cs4 Secondary crater material—Forms crater chains or clusters of small, fresh craters oriented radially to and generally related to primary craters Verdi and Jókai. Only a few major chains of secondary craters around Verdi and Jókai mapped. *Interpretation:* Nearby and farflung secondary ejecta from primary impacts
- c3 Material of craters with low, rounded, but continuous rims (FDS 156)—Floors flat, partly filled with smooth plains or intermediate plains materials. Wall terraces rare, but radial channels on wall common at Mansart; floor-wall boundary indistinct in many craters. Discontinuous field of secondary craters common. Moderate number of superposed craters
- cp3 Central peak material of c<sub>3</sub> craters—Same as cp<sub>4</sub> except occurs within c<sub>3</sub> craters. Peaks either single or multiple
- cf3 Crater floor material of c<sub>3</sub> craters—Same as cf<sub>4</sub> except occurs within c<sub>3</sub> craters
- c2 Material of pan-shaped craters with low rims covered with superposed primary and secondary craters (FDS 165)—Degraded wall terraces. Crater floor flooded with intercrater plains and smooth plains materials. No visible secondary craters
- cp2 Central peak material of c<sub>2</sub> craters—Same as cp<sub>3</sub> and cp<sub>4</sub> except occurs in c<sub>2</sub> crater Turgenev
- c1 Material of flat-floored craters with no central peak and with low, discontinuous rims (FDS 164)—No wall structure; no field of secondary craters. Crater floor flooded with smooth plains and intercrater plains materials. *Interpretation of units c<sub>3</sub> through c<sub>1</sub>* Materials of impact craters displaying various stages of degradation and infilling. Bimodal morphologic classification of craters >100 km and <100 km after McCauley and others (1981)
- cg Material of ghost craters—Cannot be dated by usual sequence of degradation; rounded rims of intercrater plains material

embayed by smooth plains material (FDS 162). Age may range from  $c_1$  to late  $c_3$ . *Interpretation:* Material of crater rims, including overturned layers, primary and secondary crater ejecta, and superposed plains material

### CORRELATION OF MAP UNITS

PLAINS MATERIAL	BASIN AND CRATER MATERIALS					
<div style="border: 1px solid black; padding: 2px; margin-bottom: 2px; background-color: #f8d7da;">ps</div> <div style="border: 1px solid black; padding: 2px; margin-bottom: 2px; background-color: #f4cccc;">psi</div> <div style="border: 1px solid black; padding: 2px; background-color: #fce4d6;">pi</div>	Caloris event	<div style="border: 1px solid black; padding: 2px; background-color: #d9ead3;">c<sub>4</sub></div> <div style="border: 1px solid black; padding: 2px; background-color: #cfe2f3;">c<sub>3</sub></div> <div style="border: 1px solid black; padding: 2px; background-color: #fce4d6;">c<sub>2</sub></div> <div style="border: 1px solid black; padding: 2px; background-color: #d9ead3;">c<sub>1</sub></div>	<div style="border: 1px solid black; padding: 2px; background-color: #d9ead3;">cp<sub>4</sub></div> <div style="border: 1px solid black; padding: 2px; background-color: #cfe2f3;">cp<sub>3</sub></div> <div style="border: 1px solid black; padding: 2px; background-color: #fce4d6;">cp<sub>2</sub></div>	<div style="border: 1px solid black; padding: 2px; background-color: #d9ead3;">cf<sub>4</sub></div> <div style="border: 1px solid black; padding: 2px; background-color: #cfe2f3;">cf<sub>3</sub></div>	<div style="border: 1px solid black; padding: 2px; background-color: #d9ead3;">cr<sub>4</sub></div>	<div style="border: 1px solid black; padding: 2px; background-color: #d9ead3;">cs<sub>4</sub></div> <div style="border: 1px solid black; padding: 2px; background-color: #d9ead3; margin-top: 10px;">cg</div>
	Goethe event					

- ?----- CONTACT—Dashed where approximately located; dotted where obliterated; queried where probable
- |— FAULT—Bar and ball on downthrown side
- LINEAMENT—Probably a fault with no vertical relief or a fault of uncertain displacement. May include unresolved crater chains of secondary impact origin
- ◆— NARROW TO BROAD RIDGE—Symbol on ridge crest. Interpreted within smooth plains material mare-type wrinkle ridge
- ▼----- RIDGE SCARP, LINEAR TO ARCUATE—Line marks base of slope. Barb points downslope; dotted where concealed. Interpreted within smooth plains material as distal edge of lava flow
- ▲— FISSURE OR TROUGH OF STRUCTURAL ORIGIN, LINEAR TO ARCUATE—Barbs point downslope
-  CRATER RIM CREST
-  CRATER RIM CREST, GREATLY SUBDUED OR BURIED—In Borealis Planitia and Goethe Basin, symbol represents ghost craters
- CRESTLINE OF GOETHE BASIN—Much subdued, only approximately located
-  AREA OF BRIGHT CRATER-RAY MATERIAL—Interpreted as ejecta from very fresh impacts
-  AREA OF ANOMALOUSLY LOW ALBEDO

## INTRODUCTION

The Borealis region surrounding the north pole of Mercury contains the Goethe Basin, whose diameter of at least 400 km makes it the sixth largest impact basin observed on Mariner 10 images (Murray and others, 1974; Strom and others, 1975; Trask and Guest, 1975; Boyce and Grolier, 1977; Strom, 1977, 1979). The west half of the mapped area (between long  $100^{\circ}$  and  $190^{\circ}$  W.) is dominated by older craters of  $c_1$ ,  $c_2$ , and  $c_3$  ages and by intercrater plains material that lies between and within them. Younger crater materials of  $c_4$  age, intermediate plains material, and small patches of smooth plains material are superposed on all other units. The  $c_4$  crater Verdi, 122 km in diameter, is the largest of the younger craters. Its extensive ejecta blanket and secondary crater field are superposed on plains materials and older craters.

The east half of the mapped area (between long  $0^{\circ}$  and  $100^{\circ}$  W.) is characterized by smooth plains material (Murray and others, 1974; Trask and Strom, 1976). This unit covers vast expanses of Borealis Planitia, a depression about 1,000 km in diameter that has an irregular arcuate west boundary. This depression is located over the site(s) of one or several old impact structures (Trask and Strom, 1976; Boyce and Grolier, 1977; Strom, 1979).

In the Borealis region, Mariner 10 images are available for only the western hemisphere, from long  $0^{\circ}$  to about long  $190^{\circ}$  W. Mercury was in darkness beyond long  $190^{\circ}$  W. on March 29, 1974, when the first Mariner 10 flyby acquired the most useful photographs of the region.

Most of the photographs used for geologic mapping were acquired by the departing spacecraft during the first pass (Mercury I). The Mercury II encounter provided no usable images of the map area; two low-oblique photographs suitable for geologic mapping were acquired during the third flyby on March 17, 1975 (Davies and others, 1978, p. 31). No stereoscopic photographic pairs are available for the Borealis region.

Because the terminator was a few degrees away from the  $0^{\circ}$ - $180^{\circ}$  meridian at the time of the first encounter, photographs of the region were acquired under a wide range of lighting conditions. These conditions and the large obliquity of the photographs hampered geologic interpretation of surface materials in the map area, as they did in the Kuiper (De Hon and others, 1981), Victoria (McGill and King, 1983), and Shakespeare (Guest and Greeley, 1983) quadrangles to the south.

Mercury's Equatorial plane is inclined less than  $2^{\circ}$  to its orbital plane (Klaasen, 1976; Murray and others, 1981, p. 28); its rotation period of 58.64 terrestrial days is in two-thirds resonance with its orbital period of 87.97 terrestrial days (Colombo, 1965; Colombo and Shapiro, 1966; Davies and others, 1978, p. 31). The resulting lag and orbital eccentricity create a variation of mean temperature not only with latitude, as on the Earth, but also with longitude. However, because of Mercury's relatively slow rotational period, diurnal variations in temperature probably greatly exceed mean-temperature variations along latitude and longitude, even in the high latitudes. Its pronounced orbital eccentricity (0.2563) causes the apparent solar intensity at Mercury to vary by more than a factor of 2 throughout a mercurian year (Davies and others, 1978, p. 2), corresponding to about a 20 percent change in equilibrium temperature. Further, conservation of orbital angular momentum and spin-orbit coupling cause considerable variation in the length of daylight. Dawns and sunsets are prolonged by the long transit time of the Mercurian horizon across the solar

disk, so that daylight is lengthened and nighttime reduced by several terrestrial days at sunset and vice versa at sunrise (Robert Wildey, U.S. Geological Survey, oral commun., 1982). Despite these considerations and despite the daily range in surface temperatures of several hundred degrees Kelvin, the subsurface temperature in the polar regions always remains well below freezing (Murray, 1975).

### STRATIGRAPHY

Within the Borealis region, three widespread plains units are recognized largely by their obvious differences in crater density, which is closely related to relative age (Soderblom and Boyce, 1972). From most heavily cratered (oldest) to least cratered (youngest), these units are intercrater plains material (unit pi), intermediate plains material (unit psi), and smooth plains material (unit ps). Visual identification is confirmed and refined by actual crater counts (table 1). If we use the lunar surface as a frame of reference, the crater density of Mercurian plains in the Borealis region is bracketed by that of the lunar uplands, the most heavily cratered lunar surface, and that of Oceanus Procellarum, a moderately cratered mare surface (figs. 1, 2, and 3). The curve for the lunar uplands was derived from crater counts in the region northwest of crater Tsiolkovskiy, between crater Mendeleev and Mare Smithii. The curve for the southeastern part of Oceanus Procellarum was obtained in an area centered near lat 2°00' N. and long 31°00'W., south of the crater Kunowsky. Ocean Procellarum has long been considered close to the "average lunar mare" (Hartmann, 1966, 1967); its crater density is intermediate between those of the heavily cratered Mare Tranquillitatis and the lightly cratered Mare Serenitatis.

TABLE 1.—Crater counts in the Borealis region

Stratigraphic unit	Counting area (A) (in km <sup>2</sup> )	Cumulative number (N) of craters (diameter ≥10 km) counted	Number of craters (diameter ≥10 km) per unit area (10 <sup>6</sup> km <sup>2</sup> )	Probable error $\frac{\sqrt{N}}{A}$
Smooth plains material	128,900	12	93	±27
Intermediate plains material	136,800	26	190	±37
Intercrater plains material	236,000	61	258	±30

Material of Borealis Planitia was not included in the smooth plains count because images of the area were blurred by spacecraft motion, and so reliable crater counts could not be obtained. However, smooth plains south

of lat 65° N. in the Shakespeare quadrangle, in the crater Strindberg and in Suisei Planitia, are included in these counts. Craters  $\geq 10$  km in diameter that are superposed on the material within the floors of craters Strindberg and Turgenev are included in the plots shown in figure 3.

The plains materials that lie outside Borealis Planitia are distributed in irregular belts, which are subparallel to the terminator and to one another. Eastward from long 190° W., the following belt pattern is observed: intercrater plains material, intermediate plains material, and again intercrater plains material. All three belts extend southward into the Shakespeare quadrangle (Guest and Greeley, 1983).

Distinguishing one type of plains material from another by variations in roughness and crater density is highly dependent on the resolution and lighting conditions of individual Mariner frames (Schaber and McCauley, 1980). This constraint is well documented for the Moon (Masursky and others, 1978, p. 80–81) and for Mars (Boyce and others, 1976). In the Borealis region, where intercrater and intermediate plains materials were imaged at an increasingly low sun angle close to the terminator, the number of observable small craters increase with decreasing distance from the terminator and concomitantly decreasing sun angle. This discrepancy in the apparent abundance of craters occurs only for craters that have small diameters and can be obviated by counting only craters larger than 3 km in diameter.

### **OLDER PLAINS MATERIALS**

The intercrater plains material (unit pi) is the oldest recognizable map unit in the Borealis region. It lies between large craters from about long 155° to long 190° W., and it also occurs between clusters of closely packed and overlapping large craters west of crater Gauguin and south and southeast of crater Mansart. The unit was described originally by Trask and Guest (1975), who considered it to be the most widespread unit on Mercury; Strom (1979) reported that this material covers one-third of the surface viewed by Mariner 10. The principal morphologic characteristic of the intercrater plains material is the high density of superposed craters 5 to 10 km in diameter, which are commonly shallow and elongate; probably they are secondary craters derived from nearby large primary craters that are superposed on the unit. As one group, the large craters and associated intercrater plains form some of the heavily cratered terrain defined by Trask and Guest (1975).

The relative age and nature of intercrater plains material are as uncertain in the Borealis region as they are elsewhere on Mercury. Strom (1979) noted the similarity in surficial morphologies between mercurian intercrater plains and pre-Imbrian pitted plains south-southwest of Mare Nectaris on the Moon (Wilhelms and McCauley, 1971; Scott, 1972). The pits in the lunar pre-Imbrian pitted plains are similar to the small secondaries that pepper the surface of Mercurian intercrater plains material. On the Moon, pre-Imbrian pitted plains material embays the Janssen Formation (Scott, 1972), whose base is defined as the base of the Nectarian System (Stuart-Alexander and Wilhelms, 1975). However, the crater density of the intercrater plains material in the Borealis region (fig. 1) matches that of an area on the far side of the Moon, in the region northwest of crater Tsiolkovskiy bounded by crater Mendeleev and Mare Smithii. This area is dominated by pre-Nectarian

unmantled terra and pre-Nectarian and Nectarian craters (Wilhelms and El-Baz, 1977). The similarity in crater density of intercrater plains material on Mercury and of pre-Nectarian terrain on the Moon is geologically significant, inasmuch as it shows that the oldest recognizable surfaces on both Mercury and the Moon went through similar stages of crustal cratering, but not necessarily at the same absolute geologic time. Differences in crater density as well as embayment relations in the Borealis region show that the intercrater plains material and the smoother intermediate plains material are younger than many c<sub>1</sub> craters in the area northeast of crater Turgenev, and older than smooth plains material in Borealis Planitia.

The relative age of intercrater plains material has a bearing on its origin (Strom, 1979). If very old, intercrater plains material may consist of anorthosite derived from a magma ocean such as may have existed on the Moon (Wood and others, 1970). If emplaced during later stages of mercurian evolution, it may consist of basin ejecta or lava flows. However, planetwide, the morphologic evidence for an impact origin rather than a volcanic one is not compelling (Strom, 1979). Whether or not either hypothesis is eventually substantiated, the emplacement of intercrater plains material likely began during an early stage of intense accretionary bombardment (Malin, 1976; Guest and O'Donnell, 1977) and lasted until the time of formation of intermediate plains material.

This general conclusion seems to be supported in the Borealis region by the relative scarcity of craters between 30 km and 60 km in diameter (fig. 1). This scarcity may indicate resurfacing by crater overlap and blanketing by crater ejecta or resurfacing by lava flows. Craters  $\geq 60$  km in diameter on Mercury also are relatively scarce compared to similar craters in the lunar uplands northwest of crater Tsiolkovskiy (fig. 1). The reduced density of large craters and basins on Mercury relative to the Moon could be either a function of different crater-population rates on these bodies or an effect of different crustal histories (Schaber and others, 1977).

Intermediate plains material (unit psi) has a roughness and crater density transitional between intercrater plains material and smooth plains material (fig. 2). In the Borealis region, the unit occurs in a rather extensive belt that extends from the Shakespeare quadrangle into Borealis north and northeast of Suisei Planitia. Intermediate plains material was first recognized and mapped in the Tolstoj quadrangle (Schaber and McCauley, 1980), where it primarily occurs on the floors of c<sub>1</sub>, c<sub>2</sub>, and c<sub>3</sub> craters. It was identified there by a lower crater density than that of intercrater plains material and by "a lower incidence of small bright-halo craters than are found on the smooth plains material" (Schaber and McCauley, 1980). Both characteristics are also typical of intermediate plains material in the Borealis region.

## **BASIN MATERIALS**

Goethe Basin is a large circular depression that measures approximately 400 km in diameter from rim crest to rim crest. It was not listed as an impact basin by Wood and Head (1976) because they considered the Mariner 10 photography too poor to confirm basin structures. However, most workers, beginning with Murray and others (1974, p. 174), have identified it as a basin. Goethe is bounded on its north and east sides by a gently sloping wall and discontinuous, low, hummocky rim material that may consist of ejecta deposits. These materials are similar to those occurring around the Caloris Basin in the Tolstoj quadrangle (Schaber and McCauley, 1980). On its west side, Goethe is bounded by at least three subparallel ridges or tilted

blocks, which are separated by narrow troughs partly filled with smooth plains material. If an inner concentric ring ever existed (Trask and Strom, 1976), it is buried under the smooth plains material that now extends across the basin. A narrow, concentric structural bench, in part resurfaced by smooth plains material, is recognizable at the base of a gently sloping and much degraded basin wall. Although rectilinear mountain massifs and the radially lineated facies of basin ejecta of the Caloris Croup surround the Caloris Basin (McCauley and others, 1981), similar units cannot be unambiguously recognized around the Goethe Basin (FDS 164). However, hilly and hummocky remnants resembling basin deposits and ejecta protrude above the gently sloping basin wall. They extend southwest and north of the basin beyond a much subdued, low, barely perceptible rim crest for a distance of one-half to one-third of the basin radius.

Goethe is older than the smooth plains material by which its wall, rim crest, and most of its ejecta were partly buried. The outlines of the rim crests of several adjacent craters are recognizable through the smooth plains material that partly fills the Goethe Basin (H-1 photomosaic, Davies and others, 1978, p. 28). These buried craters probably were formed on the basin floor after excavation of the basin and were subsequently flooded to their rims by smooth plains material (Strom and others, 1975). The terrain northwest of crater Depréz (FDS 160 and 164) is more hummocky than that farther south, suggesting that smooth plains material northwest of Depréz is so thin that the older and rougher topography of buried intercrater plains material protrudes through it. The density and size of ghost craters within the Goethe Basin are similar to those of the  $c_2$  craters superposed over intercrater plains material near the terminator. These ghost ( $c_2$ ) craters and the original intercrater plains material they characterize are younger than the Goethe Basin, as they were not obliterated by the impact that formed it. Therefore, Goethe may have impacted onto a surface older than intercrater material and been partly filled by this material at a later date. If so, the Goethe impact basin may be older than some intercrater plains material and large  $c_1$  craters nearby. It is also much older than the Caloris Basin, which was created during the time of formation of  $c_3$  craters (McCauley and others, 1981).

Several additional impact structures within and to the south of the Borealis region display sufficient structural detail to be called basins, even though their diameters are less than the arbitrarily chosen 200-km lower limit adopted by Murray and others (1974) for mercurian basins. The largest and oldest of these is Botticelli, a crater 140 km in diameter centered at lat  $64^\circ\text{N}$ ., long  $110^\circ\text{W}$ . Only the northernmost parts of the crater's rim and interior lie within the mapped area, but the ghost remnant of an inner ring now flooded by smooth plains material is recognized (FDS 148) farther south in the Shakespeare quadrangle. Turgenev, 110 km in diameter, is large enough to be a central-peak basin (Wood and Head, 1976), even though the peak ring probably has been concealed under smooth plains material. The rims of both Botticelli and Turgenev are covered with densely packed craters, most of which resemble the secondary craters that typically occur on intercrater plains material. Therefore, Botticelli and Turgenev are at least as old as intercrater plains material and may be equivalent in age to the Goethe impact basin. A similar argument can be advanced for the age of the Monteverdi Basin, 130 km in diameter, centered at lat  $64^\circ\text{N}$ ., long  $77^\circ\text{W}$ . in the Victoria quadrangle. The younger craters Jókai and Verdi, which have prominent central peaks and ghostlike discontinuous inner rings, probably

qualify as central-peak basins (Wood and Head, 1976). Both structures are considerably younger than the Caloris Basin.

No material similar to either the lineated or the secondary-crater facies of the Van Eyck Formation, the most distinctive and distant unit of the Caloris Group (McCauley and others, 1981), can be unambiguously identified in the Borealis region. A few rounded hills or knobs, too small to be mapped, are present; they are morphologically similar to blocks of the Odin Formation surrounding the Caloris Basin in the Shakespeare quadrangle (Guest and Greeley, 1983), and to features of the Alpes Formation around the Imbrium Basin on the Moon. Two of the most striking of these knobs are possibly 2 km long and 0.2 km across; they rise above smooth plains material that fills a much degraded, unmapped, irregular crater at 69° N., 157° W. (FDS 088). These knobs are about 1,100 km northeast of Caloris Montes and may represent Caloris Basin ejecta. Alternatively, they may be associated with crater Verdi ejecta or with lineated and secondary-crater ejecta that flare southeastward from an unnamed crater north of and adjacent to the crater Nizami. Another morphologic feature that may be related to the Caloris Basin event consists of grooves on intercrater plains material and on the southwest-facing walls of craters such as Mansart. These grooves are as much as several kilometers long and several hundred meters wide. The direction of elongation of many small secondary craters also suggests an origin related to the Caloris event.

### **YOUNGER PLAINS MATERIAL**

Smooth plains material (unit ps) forms the vast expanses of Borealis and Suisi Planitiae, as well as most basin and crater floors. It is the most extensive stratigraphic unit in the Borealis region, covering 30 percent of the mapped area. The surface of the smooth plains material is rather sparsely cratered compared to that of the intercrater plains material (figs. 3, 1). Wrinkle ridges are common. Both the floor of the Goethe Basin and the younger craters (now observed as buried craters) superposed on it are mantled by smooth plains material; the unit also fills ghost and flooded craters that are common on both Borealis and Suisi Planitiae and resemble the lunar crater Archimedes. The enormous volume of smooth plains material that must underlie Borealis Planitia in order to bury pre-existing topography, as well as the presence of the material in basin and crater floors, suggest that the smooth plains material was emplaced in a fluidized state as volcanic lava flows (Murray and others, 1974; Strom and others, 1975). Even though flow fronts cannot be unambiguously mapped on Borealis Planitia, further evidence of the unit's volcanic origin is supplied by its overlap onto intercrater plains material, best observed along the west edge of Borealis Planitia (FDS 85, 152, 153, 156, and 160).

The various types of plains material recognized on Mercury exhibit little tonal contrast. The albedo of smooth plains material is higher than that of lunar mare material (Hapke and others, 1975). The similarity in albedo between mercurian smooth plains material and lunar light plains material led Wilhelms (1976) to extend the analogy to composition: he suggested that both units consist of impact ejecta similar to the lunar Cayley Formation sampled by Apollo 16. Wilhelms (1976, p. 556) even hypothesized that the source basin for material of the extensive plains of Borealis Planitia "could well be lurking in the darkness beyond the terminator." A fuller discussion of the problem is given by Strom (1979).

## CRATER MATERIALS

In the Borealis region, craters are mapped according to the fivefold classification proposed by McCauley and others (1981), which determines Mercurian crater ages on the basis of crater diameter and morphologic degradation. Craters less than about 30 km in diameter are not mapped. All basins between 100 and 200 km in diameter (including those that have central peaks and peak rings) are mapped as craters. Criteria used to determine impact structures are morphologic crater components such as rays, secondary rays, hummocky rims, various facies of crater ejecta, crater geometry and structure, or a combination of these. The Verdi crater is defined as the type example of a young, large, c5 crater by McCauley and others (1981), but was mapped as a c4 crater in the Shakespeare quadrangle (Guest and Greeley, 1983) prior to the release of McCauley and others' crater classification. For this reason, the Verdi crater is also mapped as a c4 crater in the Borealis region.

No rayed craters  $\geq 30$  km in diameter were observed in the mapped area, but many moderately bright and diffuse rays extend across smooth plains material or occur as halos around very small craters in Borealis Planitia. The most conspicuous of these are indicated on the map. A train of northeast-trending discontinuous rays, which extends across Borealis Planitia as far as the Goethe Basin, may radiate from small unnamed and unmapped rayed craters near the south edge of the map area. The relative scarcity of small bright-halo craters on intermediate plains material, perhaps due to unique physical properties of this material, was first noted in the Tolstoj quadrangle (Schaber and McCauley, 1980); this scarcity is also characteristic of the unit in the Borealis region.

The reduced ballistic range on Mercury compared to the Moon is caused by Mercury's stronger gravitational field (Gault and others, 1975; Strom, 1979; McCauley and others, 1981). This phenomenon, which results in a reduced dispersion of ejecta and secondary craters, is best observed within the Borealis region around craters Verdi (Gault and others, 1975; Trask and Guest, 1975) and Depréz. Slight differences between mercurian and lunar crater morphologies are unrelated to differences in the Mercurian and lunar gravitational fields (Cintala and others, 1977; Malin and Dzurisin, 1977, 1978; Strom, 1979). Instead, the morphologic components of crater interiors and the abundance of central peaks and terraces on both bodies seem to be related to the physical properties of the target material (Cintala and others, 1977; Smith and Hartnell, 1978; Strom, 1979).

The clusters of closely packed and overlapping large c2 and c3 craters west of crater Gauguin and east of crater Mansart, together with nearby isolated craters and surrounding material, were mapped by Trask and Guest (1975) as heavily cratered terrain. According to them, many of the small craters superposed on the intercrater areas may be secondaries from the large c2 and c3 craters. They also noted that the interiors of these large craters are filled with material that is less cratered, smoother, and therefore younger than the intercrater plains material. We have mapped these craters individually and have mapped the material between them as intercrater plains or intermediate plains materials.

Two types of ghost craters occur in the Borealis region; both are nearly obliterated by smooth plains material. In one type (unit cg) found along the northwest border of Suisei Planitia (Guest and Greeley, 1983), only the uppermost parts of walls and rims protrude above smooth plains material. Ghost craters of this type display rounded rim crests that are densely

cratered with secondaries, a feature typical of the rough surface of intercrater plains material. These craters are floored by smooth plains material and are therefore older than it; a similar relation occurs on the Moon, where the crater Archimedes is seen to be older than the mare material it contains. Another type of ghost crater, common in Borealis Planitia, is recognized only by an irregular or thin outline of a rim crest under a thin mantle of smooth plains material; the buried rim crest is shown on the map. The polygonal ghost crater centered at lat 82.5° N., long 100° W., northwest of Depréz, is a transitional form between these two types. Ghost craters in the Borealis region are estimated to be of c<sub>1</sub> to c<sub>3</sub> age on the basis of degradation of their rim crests, relative density of superposed craters on their rims, and embayment by smooth plains material.

Polar darkening is generally lacking on Mercury (Hapke, 1977), but darkening in restricted areas may be due to vapor-phase deposition accompanying micrometeorite impacts (Hapke, 1977; Strom, 1979). In the Borealis region, surface darkening affects some crater floors, and low-albedo areas are mapped in both intermediate plains and smooth plains materials. The low-albedo plains are marginal to the borders of Borealis and Suisei Planitiae, which suggests that darkening may be due to internal volatile materials escaping along the fractured margins of unrecognized buried or very degraded basins.

## STRUCTURE

One of the major differences between the mercurian and lunar surfaces is “the widespread distribution [on Mercury] of lobate scarps which appear to be thrust or reverse faults resulting from a period of crustal compression...” (Strom, 1979, p. 10–11). These scarps are unique structural landforms that were noted soon after the acquisition of Mariner 10 photographs. Murray and others (1974) described them as having a sinuous outline, a slightly lobate front, and a length of more than 500 km. A more detailed description is given by Strom and others (1975). Dzurisin (1978) classified these scarps, differentiating between intercrater and intracrater scarps (a scheme adopted in mapping the Borealis region) in an attempt to understand the tectonic and volcanic history of Mercury. Melosh (1977) and Melosh and Dzurisin (1978) proposed a planetary grid composed of conjugate northeast- and northwest-trending shear fractures formed by the stresses of tidal despinning early in mercurian history. They thought that these fractures were later modified, and predicted that east-trending normal faults caused by tensional stresses would be found in the polar regions. In a later report, Pechmann and Melosh (1979, p. 243) stated that “the NE and NW trends become nearly N-S in the polar regions.”

The northwest-trending component of the postulated global grid of fractures is markedly absent in the Borealis region. Northeast-trending scarps and troughs are conspicuous, however, across intercrater plains material and in crater fill (smooth plains material) between the 155° and 185° meridians, and from crater Van Dijck northward to crater Purcell and beyond. The scarps tend to be straight in intercrater plains material, but become notably lobate in crater fill (for example, within Saikaku). This set of northeast-trending scarps and troughs, and another set of north-trending scarps and troughs within and north of crater Van Dijck, probably follow zones of structural weakness in the mercurian crust. Ancient fractures that were reactivated by later impacts may have first provided the conduits for crater fill (smooth plains material) and later been propagated upward

through the fill. That these ridges, scarps, and troughs are parts of a global grid of fractures cannot be stated conclusively because of their proximity to the terminator and the lack of photographic coverage beyond the 190° meridian. Some scarps probably were formed by normal faulting of the smooth plains material that covers some crater floors, as in the Kuiper quadrangle (Scott and others, 1980). We cannot, however, determine whether most lineaments are internal or are parts of a faulted and lineated facies associated with a nearby but unphotographed impact basin. Melosh (1977) predicted that normal east-trending faults would form in high Mercurian latitudes as a result of slight crustal shortening. His predicted faults may be represented by a generally east-northeast-trending scarp and a lineament that cut across intermediate plains material and the crater Jókai between the 125° and 155° meridians. The north pole is too close to the terminator to detect the presence or absence of a “polygonal arrangement without preferred orientation,” as predicted by Melosh and Dzurisin (1978, p. 233).

Arcuate and radial lineaments that might result from tectonic adjustments of the Mercurian crust, following excavation of very large multiring impact basins such as the one postulated under Borealis Planitia (Trask and Strom, 1976; Boyce and Grolier, 1977; Strom, 1979), were not unambiguously identified in the Borealis region. On one hand, some ridges on the surface of the smooth plains material in Borealis Planitia may be of structural (internal) origin; this type of ridge elsewhere on Mercury has been ascribed to compression and a slight shortening of the crust (Strom and others, 1975; Melosh, 1977; Melosh and Dzurisin, 1978). On the other hand, the wrinklelike sinuous ridge along the northeast border of the Goethe Basin, together with the outward-facing concentric scarps along its periphery, may represent the fronts of lava flows that are associated with the development of a structural moat between the basin fill and the wall. The latter interpretation supports the view that impact craters and basins on Mercury, as on the Moon (Schultz, 1977) and Mars, “have played a dominant role in controlling the surface expression of igneous activity” (Schultz and Glicken, 1979, p. 8033). Slow, long-lasting isostatic adjustment of the basin floor may have continued well after the emplacement of the basin fill, a structural situation similar to that of crater Posidonius on the Moon (Schaber and others, 1977, Schultz, 1977).

In Borealis Planitia, however, most of the ridges are of external origin. They appear either to outline the rim crests of subjacent ghost craters that are lightly mantled by smooth plains material or to be lava flow fronts. The map shows the rim crests of 20 ghost craters, ranging in diameter from 40 to 160 km, that are buried under the smooth plains material of Borealis Planitia, which material is coextensive with the fill covering the floor of the Goethe Basin. In addition, ejecta from the crater Depréz extend more than 40 km eastward beyond a circular scarp that may represent the rim crest of a buried crater 170 km in diameter (FDS 156, 160) or, more likely, the front of lava flows. The size and density of these ghost craters suggest that, prior to emplacement of smooth plains material, the original heavily cratered surface of Borealis Planitia—which may have been the cratered floor of a very large multiring impact basin—and the cratered floor of the Goethe Basin were similar in composition and age to the intercrater plains material of the highlands to the west. Many scarps in Borealis Planitia are subconcentric to the rim of the Goethe Basin and have steeper slopes that face away from it, suggesting that they represent the fronts of lava flows that resurfaced

extensive areas of heavily cratered terrain (intercrater or older plains material).

## **GEOLOGIC HISTORY**

Five periods were postulated by Murray and others (1975) to constitute the history of Mercury's surface: (1) accretion and differentiation; (2) terminal bombardment; (3) formation of the Caloris Basin; (4) flooding of that basin and other areas; and (5) light cratering on the smooth plains. Only the periods following accretion are directly interpretable within the Borealis region.

Intercrater plains material, which may be a reworked and mixed aggregate of impact and volcanic deposits, was emplaced over a long period that extended past the creation of the Goethe Basin and many smaller c<sub>1</sub> and c<sub>2</sub> basins and craters. The scarps and troughs that trend across intercrater plains material may indicate an early compressional episode that followed even earlier expansion and differentiation of the crust.

The size and density of ghost craters that are detectable under the smooth plains material in the interior of the Goethe Basin are indicative of an original basin floor much modified by cratering and emplacement of intercrater materials prior to the emplacement of intermediate and smooth plains materials. This interpretation implies, therefore, that the formation of the Goethe Basin predated or occurred soon after the emplacement of intercrater plains material had begun. The relative similarity in albedo of the Mercurian plains, whether formed of intercrater, intermediate, or smooth plains materials, also suggests a similarity in chemical composition and possibly in mode of emplacement of plains materials. The high crater density of intercrater and intermediate plains materials makes it likely, however, that the original rock types of these two units (whether basalt, impact melt, or impact breccia) were modified considerably by further brecciation following emplacement.

Morphologic and stratigraphic evidence from the Shakespeare and Tolstoj quadrangles shows that the Caloris event occurred late in the time span during which c<sub>3</sub> craters were formed. As indicated above, our interpretation is that the Goethe Basin is older than some intercrater material and large c<sub>1</sub> craters and, therefore, is considerably older than the Caloris Basin. Emplacement of the smooth plains material of Borealis Planitia during several or many episodes resulted in resurfacing and smoothing of the original material of the Goethe Basin and its surroundings for hundreds of kilometers.

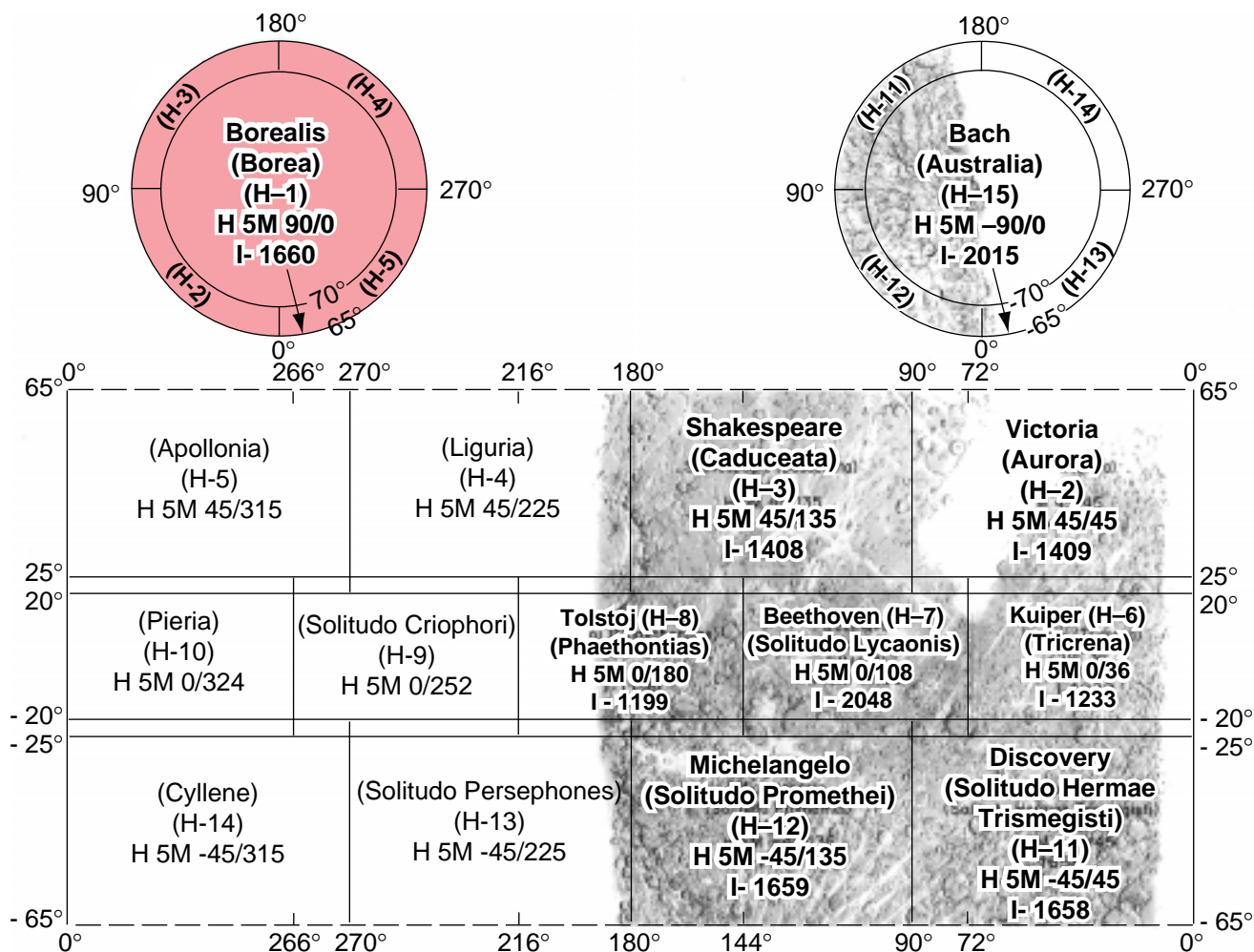
The mercurian surface reached its present configuration several billion years ago (Solomon, 1978). It has been only slightly altered since by the impacts that created c<sub>4</sub> craters, which are ubiquitously superposed on all other deposits. Generalized summaries of the history of Mercury have been given by Guest and O'Donnell (1977), Davies and others (1978), and Strom (1979).

## REFERENCES

- Boyce, J. M., Dial, A. L., and Masursky, Harold, 1976, The optimal sun angle for obtaining photographs of martian surface features from orbit: U.S. Geological Survey Interagency Report: *Astrogeology* 78, 8 p.
- Boyce, J. M., and Grolier, M. J., 1977, The geology of the Goethe (H-1) quadrangle of Mercury, *in* Arvidson, Raymond, and Wahmann, Russell, eds., Reports of planetary geology program, 1976–1977: National Aeronautics and Space Administration Technical Memorandum X-3511, p. 237.
- Cintala, M. J., Wood, C. A., and Head, J. W., 1977, The effects of target characteristics on fresh crater morphology: Preliminary results for the moon and Mercury: Lunar Science Conference, 8th, Houston, 1977, Proceedings, p. 3409–3425, 4 figs., 3 tables.
- Colombo, Giuseppe, 1965, Rotational period of the planet Mercury: *Nature*, v. 208, no. 5010, p. 575.
- Colombo, Giuseppe, and Shapiro, I. I., 1966, The rotation of the planet Mercury: *Astrophysical Journal*, v. 145, p. 296–307.
- Davies, M. E., Dwornik, S. E., Gault, D. E., and Strom, R. G., 1978, Atlas of Mercury: National Aeronautics and Space Administration Special Publication SP-423, 128 p.
- De Hon, R. A., Scott, D. H., and Underwood, J. R., Jr., 1981, Geologic map of the Kuiper quadrangle of Mercury; U.S. Geological Survey Miscellaneous Investigations Series Map I-1233, scale 1:5,000,000.
- Dzurisin, Daniel, 1978, The tectonic and volcanic history of Mercury as inferred from studies of scarps, ridges, troughs, and other lineaments: *Journal of Geophysical Research*, v. 83, no. B10, p. 4883–4906.
- Gault, D. E., Guest, J. E., Murray, J. B., Dzurisin, Daniel, and Malin, M. C., 1975, Some comparisons of impact craters on Mercury and the Moon: *Journal of Geophysical Research*, v. 80, no. 17, p. 2444–2460.
- Guest, J. E., and Greeley, Ronald, 1983, Geologic map of the Shakespeare quadrangle of Mercury: U.S. Geological Survey Miscellaneous Investigations Series Map I-1408, scale 1:5,000,000.
- Guest, J. E., and O'Donnell, W. P., 1977, Surface history of Mercury: A review: *Vistas in Astronomy*, v. 20, p. 273–300.
- Hapke, Bruce, 1977, Interpretations of optical observations of Mercury and the Moon: *Physics of the Earth and Planetary Interiors*, v. 15, p. 264–274.
- Hapke, Bruce, Danielson, G. E., Jr., Klaasen, Kenneth, and Wilson, Lionel, 1975, Photometric observations of Mercury from Mariner 10: *Journal of Geophysical Research*, v. 80, no. 17, p. 2431–2443
- Hartmann, W. K., 1966, Early lunar cratering: *Icarus*, v. 5, no.4, p. 406–418.
- \_\_\_\_\_ 1967, Lunar crater counts, III: Post mare and “Archimedian” variations: *Lunar and Planetary Laboratory, Communication no. 116*, v. 7, pt. 3, p. 125–129.
- Klaasen, K. P., 1976, Mercury’s rotation axis and period: *Icarus*, v. 28, no. 4, p. 469–478.

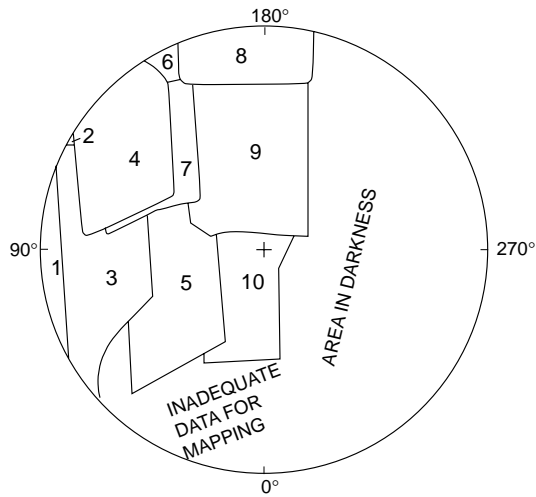
- Malin, M. C., 1976, Observations of intercrater plains on Mercury: *Geophysical Research Letters*, v. 3, no. 10, p. 581–584.
- Malin, M. C., and Dzurisin, Daniel, 1977, Landform degradation on Mercury, the Moon, and Mars: Evidence from crater depth/diameter relationships: *Journal of Geophysical Research*, v. 82, no. 2, p. 376–388, 7 figs., 7 tables.
- \_\_\_\_\_, 1978, Modification of fresh crater landforms: Evidence from the Moon and Mercury: *Journal of Geophysical Research*, v. 83, no. B1, p. 233–243.
- Masursky, Harold, Colton, G. W., and El-Baz, Farouk, eds., 1978, *Apollo over the Moon: A view from orbit*: National Aeronautics and Space Administration Special Publication 362, 255 p.
- McCauley, J. F., Guest, J. E., Schaber, G. G., Trask, N. J., and Greeley, Ronald, 1981, Stratigraphy of the Caloris Basin, Mercury: *Icarus*, v. 47, no. 2, p. 184–202.
- McGill, G. E., and King, E. A., 1983, Geologic map of the Victoria quadrangle of Mercury: U.S. Geological Survey Miscellaneous Investigations Series Map I-1409, scale 1:5,000,000.
- Melosh, H. J., 1977, Global tectonics of a despun planet: *Icarus*, v. 31, no. 2, p. 221–243.
- Melosh, H. J., and Dzurisin, Daniel, 1978, Mercurian global tectonics: A consequence of tidal despinning?: *Icarus*, v. 35, no. 2, p. 227–236.
- Murray, B. C., Belton, J. J. S., Danielson, G. E., Davies, M. E., Gault, D. E., Hapke, Bruce, O’Leary, Brian, Strom, R. G., Suomi, Verner, and Trask, Newell, 1974, Mercury’s surface: Preliminary description and interpretation from Mariner 10 pictures: *Science*, v. 185, no. 4146, p. 169–179.
- Murray, B. C., Malin, M. C., and Greeley, Ronald, 1981, *Earthlike planets*: San Francisco, W. H. Freeman and Co., 387p.
- Murray, B. C., Strom, R. G., Trask, N. J., and Gault, D. E., 1975, Surface history of Mercury: Implications for terrestrial planets: *Journal of Geophysical Research*, v. 80, no. 17, p. 2508–2514.
- Pechmann, J. B., and Melosh, H. J., 1979 Global fracture patterns of a despun planet: Application to Mercury: *Icarus*, v. 38, no. 2, p. 243–250.
- Schaber, G. G., Boyce, J. M., Trask, N.J., 1977, Moon-Mercury: Large impact structures, isostasy, an average crustal viscosity: *Physics of the Earth and Planetary Interiors*, v. 15, nos. 2–3, p. 189–201.
- Schaber, G. G., and McCauley, J. F., 1980, Geologic map of the Tolstoj quadrangle of Mercury: U.S. Geological Survey Miscellaneous Investigations Series Map I-1199, scale 1:5,000,000.
- Schultz, P. H., 1977, Endogenic modification of impact craters on Mercury: *Physics of the Earth and Planetary Interiors*, v. 15, nos. 2–3, p. 202–219.
- Schultz, P. H., and Gicken, Harry, 1979, Impact crater and basin control of igneous processes on Mars: *Journal of Geophysical Research*, v. 84, no. B14, p. 8033–8047.
- Scott, D. H., 1972, Geologic map of the Maurolycus quadrangle of the Moon: U.S. Geological Survey Miscellaneous Investigations Map I-695, scale 1:1,000,000.

- Scott, D. H., Underwood, J. R., Jr., and De Hon, R. A., 1980, Normal faults on Mercury: Example in the Kuiper quadrangle, *in* Reports of planetary programs, 1979–1980: National Aeronautics and Space Administration Technical Memorandum 81776, p. 28–30.
- Smith, E. I., and Hartnell, J. A., 1978, Crater-size-shape profiles for the Moon and Mercury: Terrain effects and interplanetary comparisons: The Moon and the Planets, v. 19, p. 479–511, 17 figs., 3 tables, appendices.
- Soderblom, L. A., and Boyce, J. M., 1972, Relative age of some near-side and far-side terra plains based on Apollo 16 metric photography: Apollo 16 Preliminary Report: National Aeronautics and Space Administration Special Publication 315, p. 29.3–29.6.
- Solomon, S. C., 1978, On volcanism and thermal tectonics on one-plate planets: Geophysical Research Letters, v. 5, no. 6, p. 461–464, 3 figs.
- Strom, R. G., 1977, Origin and relative age of lunar and mercurian intercrater plains: Physics of the Earth and Planetary Interiors, v. 15, nos. 2–3, p. 156–172.
- \_\_\_\_\_, 1979, Mercury: A post-Mariner 10 assessment: Space Science Reviews, v. 24, no. 1, p. 3–70.
- Strom, R. G., Trask, N. J., and Guest, J. E., 1975, Tectonism and volcanism on Mercury: Journal of Geophysical Research, v. 80, no. 17, p. 2478–2507.
- Stuart-Alexander, D. E., and Wilhelms, D. E., 1975, The Nectarian System: A new lunar time-stratigraphic unit: U.S. Geological Survey Journal of Research, v. 3, no. 1, p. 53–58.
- Trask, N. J., and Guest, J. E., 1975, Preliminary geologic terrain map of Mercury: Journal of Geophysical Research, v.80, no.17, p.2461–2477.
- Trask, N. J., and Strom, R. G., 1976, Additional evidence of mercurian volcanism: Icarus, v. 28, no. 4, p. 559–563.
- Wilhelms, D. E., 1976, Mercurian volcanism questioned: Icarus, v. 28, no. 4, p. 551–558.
- Wilhelms, D. E., and El-Baz, Farouk, 1977, Geologic map of the east side of the Moon: U.S. Geological Survey Miscellaneous Investigations Series Map I-948, scale 1:5,000,000.
- Wilhelms, D. E., and McCauley, J. F., 1971, Geologic map of the near side of the Moon: U.S. Geological Survey Miscellaneous Geologic Investigations Map I-1703, scale 1:5,000,000.
- Wood, C. A., and Head, J. W., 1976, Comparison of impact basins on Mercury, Mars and the Moon: Lunar Science Conference, 7th, Houston, 1977, Proceedings, p. 3629–3651.
- Wood, J. A., Dickey, J. S., Marvin, U. B., and Powell, B. N., 1970, Lunar anorthosites and a geophysical model of the Moon: Apollo 11 Lunar Science Conference, Houston, 1970, Proceedings, v. 1, p. 965–988.



ARRANGEMENT OF MAP SHEETS ON MERCURY

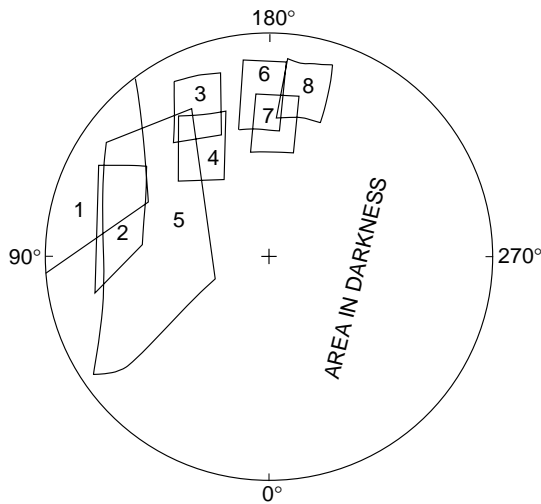
The provisional name "Goethe" was changed to "Borealis," and the provisional name "Tir" was changed to "Tolstoj" by the International Astronomical Union in 1976 (IAU, 1977). These provisional names appeared on earlier editions of this index map and on the shaded relief map of Tolstoj (H-8) quadrangle. The number preceded by I refers to published geologic map.



Index No.	FDS No.
1	148
2	149
3	152
4	157
5	160
6	162
7	161
8	166
9	165
10	164

#### INDEX OF MARINER 10 PICTURES

The mosaic used to control the positioning of the features on this map was made with the Mariner 10 pictures outlined above.



Index No.	FDS No.
1	153
2	85
3	88
4	84
5	156
6	87
7	83
8	86

#### SUPPLEMENTAL SOURCE INDEX

The Mariner 10 pictures outlined above were used to provide additional detail on the map but were not used on the controlled mosaic.

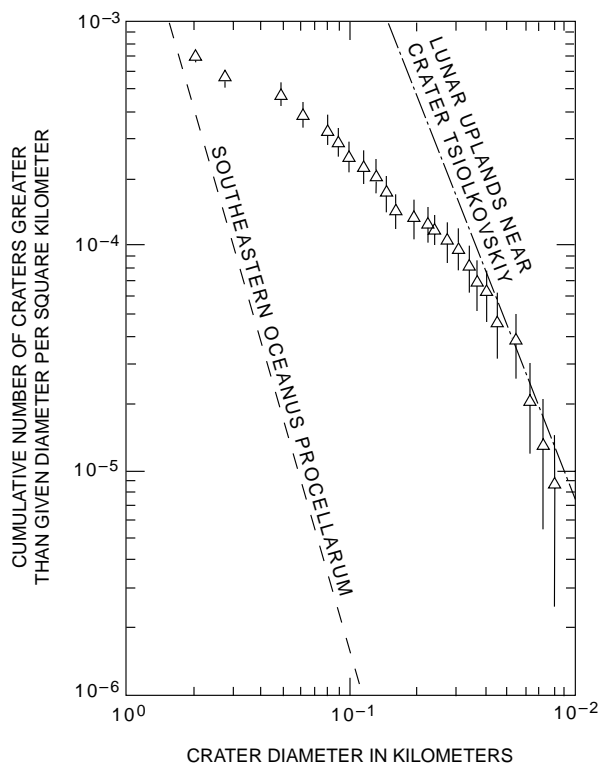


FIGURE 1.—Log-log plot of cumulative size-frequency distribution of craters in heavily cratered intercrater plains material in the Borealis region within a belt bordering terminator and within an east-trending area east of crater Jókai. Note decrease in slope of the Mercurian curve where craters are smaller than 30 km and larger than 60 km. Also note coincidence of the abundance of craters in the 55- to 65-km-diameter range with the curve for lunar pre-Nectarian terra northwest of crater Tsiolkovskiy. Intercrater plains material has been more heavily impacted by craters larger than 4 km in diameter (and is, therefore, older) than southeastern part of Oceanus Procellarum, the near-average lunar mare. (See section on stratigraphy.) Bars represent standard error or deviation ( $\pm \sqrt{\frac{N}{A}}$ , where N=cumulative number of craters greater than given diameter per square kilometer and A=unit area). Crater counts and curves by Arthur L. Dial, Jr.

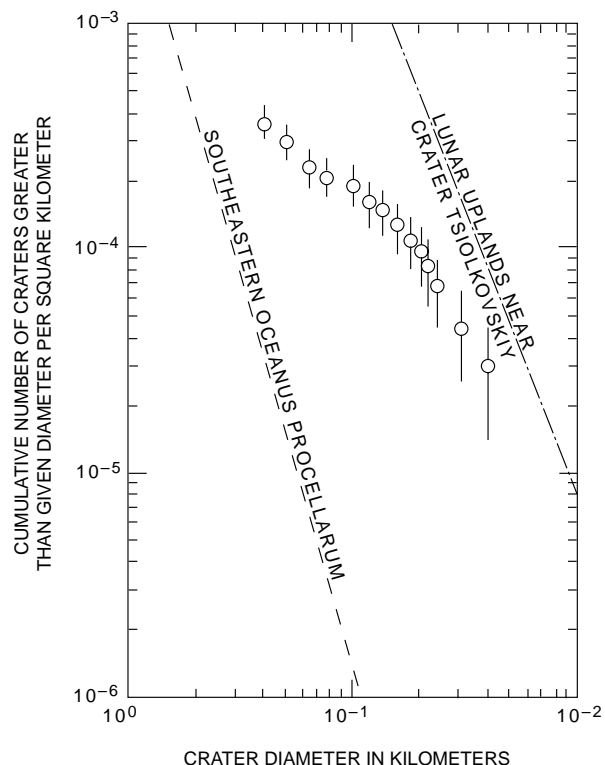


FIGURE 2.—Log-log plot of cumulative size-frequency distribution of craters in intermediate plains material within and adjoining the Borealis region. Crater density is intermediate between those of intercrater plains and smooth plains materials. (For explanation of lunar curves, see fig. 1 and section on stratigraphy). Bars represent standard error or deviation ( $\pm \sqrt{\frac{N}{A}}$ , where N=cumulative number of craters greater than given diameter per square kilometer and A=unit area). Crater counts and curves by Arthur L. Dial, Jr.

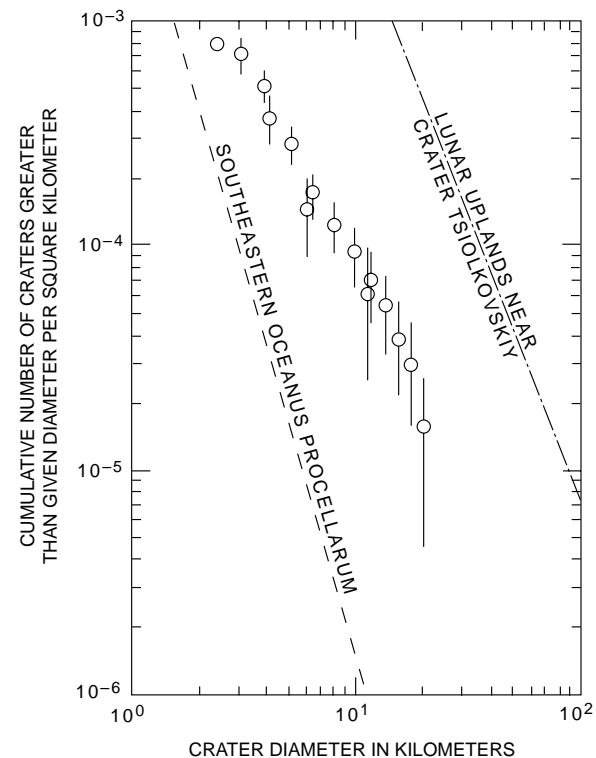


FIGURE 3.—Log-log plot of cumulative size-frequency distribution of craters in smooth plains material west of Borealis Planitia in and adjoining the Borealis region. (This material includes the very smooth plains material mapped in the Shakespeare quadrangle by Guest and Greeley, 1983.) Open circles represent counts on the floors of craters Strindberg (in the Shakespeare quadrangle) and Turgenev. Note that the curve follows the -2 distribution function for craters having diameters between 3 and 20 km. Smooth plains material is less cratered than intermediate plains material (fig. 2), and its curve lies between those of southeastern part of Oceanus Procellarum (near-average lunar mare) and lunar uplands. Bars represent standard error or deviation ( $\pm \sqrt{\frac{N}{A}}$ , where N=cumulative number of craters greater than given diameter per square kilometer and A=unit area). Crater counts and curves by Arthur L. Dial, Jr.

## NOTES ON BASE

This map sheet is one of a series covering that part of the surface of Mercury that was illuminated during the Mariner 10 encounters (Davies and Batson, 1975). The source of map data was the Mariner 10 television experiment (Murray, 1975).

## ADOPTED FIGURE

The map projections are based on a sphere with a radius of 2439 km.

## PROJECTION

The polar stereographic projection is used for this sheet, with a scale of 1:4,290,000 at lat 65°. Latitudes are based on the assumption that the spin axis of Mercury is perpendicular to the plane of the orbit. Longitudes are positive westward in accordance with the usage of the International Astronomical Union (IAU, 1971). Meridians are numbered so that a reference crater named Hun Kal (lat 0.6° S.) is centered on long 20 (Murray and others, 1974; Davies and Batson 1975).

## CONTROL

Planimetric control is provided by photogrammetric triangulation using Mariner 10 pictures (Davies and Batson, 1975). Discrepancies between images in the base mosaic and computed control-point positions appear to be less than 2 km, except for the area east of about long 90°. Pictures of this area are so foreshortened that accurate map transformations were not possible. Since the base mosaic was controlled by a later iteration of the control net, discrepancies as large as 20 km exist between this sheet and the Victoria (H-2) and Shakespeare (H-3) sheets to the south. These discrepancies were adjusted within the area north of lat 70°.

## MAPPING TECHNIQUES

Mapping techniques are similar to those described by Batson (1973a, 1973b). A mosaic was made with pictures that had been digitally transformed to the polar stereographic projection. Shaded relief was copied from the mosaics and portrayed with uniform illumination with the sun to the west. Many Mariner 10 pictures besides those in the base mosaic were examined to improve the portrayal. The shading is not generalized and may be interpreted with nearly photographic reliability (Inge, 1972; Inge and Bridges, 1976).

Shaded relief analysis and representation were made by J. L. Inge.

## NOMENCLATURE

All names on this sheet are approved by the International Astronomical Union (IAU, 1977).

H-1: Abbreviation for Mercury (Hermes) sheet number 1.  
H 5M 90/0 G: Abbreviation for Mercury (Hermes) 1:5,000,000 series; center of sheet, lat 90° N., long 0°; geologic map, G.

## REFERENCES

- Batson, R. M., 1973a, Cartographic products from the Mariner 9 mission: *Journal of Geophysical Research*, v. 78, no. 20, p. 4424–4435.
- \_\_\_\_\_, 1973b, Television cartography: U.S. Geological Survey open-file report, *Astrogeology* 58, 35 p.
- Davies, M. E., and Batson, R. M., 1975, Surface coordinates and cartography of Mercury: *Journal of Geophysical Research*, v. 80, no. 17, p. 2417–2430.
- Inge, J. L., 1972, Principles of lunar illustration: Aeronautical Chart and Information Center Reference Publication RP-72-1, 60 p.
- Inge, J. L., and Bridges, P. M., 1976, Applied Photointerpretation for airbrush cartography: *Photogrammetric Engineering and Remote Sensing*, v. 42 no. 6, p. 749–760.
- International Astronomical Union, 1971, Commission 16: Physical study of planets and satellites, *in* 14th General Assembly, Brighton, 1970, Proceedings: International Astronomical Union Transactions, v. 14B, p. 105–108.
- \_\_\_\_\_, 1977, Working Group for Planetary System Nomenclature, *in* 16th General Assembly, Grenoble, 1976, Proceedings: International Astronomical Union Transactions, v. 16B, p. 321–325, 330–332, 351–355.
- Murray, B. C., 1975, The Mariner 10 pictures of Mercury—an overview: *Journal of Geophysical Research*, v. 80, no. 17, p. 2342–2344.
- Murray, B. C., Belton, M. J. S., Danielson, G. E., Davies, M. E., Gault, D. E., Hapke, Bruce, O’Leary, Brian, Strom, R. G., Soumi, Verner, and Trask, Newell, 1974, Mercury’s surface: Preliminary description and interpretation from Mariner 10 pictures: *Science*, v. 185, no. 4146, p. 169–179.